Available online at www.sciencedirect.com

ScienceDirect

journal homepage: www.elsevier.com/locate/he

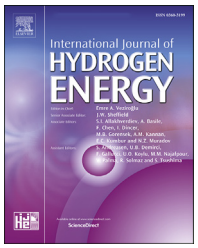

Synthesis of cobalt and nitrogen co-doped carbon nanotubes and its ORR activity as the catalyst used in hydrogen fuel cells

Hongwei Zhao [a], *Tianyu Xing* [c], *Lixiang Li* [a,*], *Xin Geng* [a], *Ke Guo* [b], *Chengguo Sun* [a], *Weimin Zhou* [a], *Haiming Yang* [a], *Renfeng Song* [b], *Baigang An* [a,**]

[a] *Institute of Energy Materials and Electrochemistry Research, University of Science and Technology Liaoning, Ashan 114051, China*

[b] *Ansteel Mining Engineering Corporation, Anshan 114004, China*

[c] *Hengli Petrochemical (Dlian) Ltd, Dlian 116318, China*

ARTICLE INFO

Article history:
Received 9 February 2019
Received in revised form
22 March 2019
Accepted 28 March 2019
Available online 22 April 2019

Keywords:
Oxygen reduction reaction
Nitrogen doped
Carbon nanotubes
Cobalt
Synergistic effect

ABSTRACT

In hydrogen fuel cells, the sluggish oxygen reduction reaction (ORR) requires the catalysts used. Unfortunately, the precious platinum based catalysts still exhibit the best ORR activity in the commercial hydrogen fuel cells. Therefore, developing non-precious metal catalysts ORR become an important aspect for the utilization of hydrogen energy by using hydrogen fuel cells to develop non-precious catalysts and understand their active sites of ORR, herein the cobalt and nitrogen co-doped CNTs, nitrogen-doped CNTs and cobalt doped CNTs were prepared, respectively, and their catalytic properties toward ORR were tested and compared. The surface composition, microstructure and ORR performance of the samples were examined by X-ray diffraction (XRD), X-ray photoelectron spectroscopy (XPS), pore/specific surface analyzer and electrochemical methods. The results demonstrate that as the catalyst, the cobalt and nitrogen co-doped CNTs owns the highest ORR limiting current density, the most positive ORR onset potential and the largest transfer electron number close to four, and thus exhibits the better ORR catalytic performance compared to the other two samples of the nitrogen-doped CNTs and the cobalt doped CNTs. The good ORR performance of cobalt and nitrogen co-doped CNTs can be attributed to its active sites of nitrogen containing functional groups, cobalt or cobalt oxides, Co-N_x structure, and the synergistic effect of these sites on ORR.

* *Corresponding author.*
** *Corresponding author.*
E-mail addresses: lxli2005@126.com (L. Li), bgan@ustl.edu.cn (B. An).
https://doi.org/10.1016/j.ijhydene.2019.03.271

Introduction

Hydrogen fuel cells can convert chemical energy into electricity through the electrochemical oxidation of hydrogen and the electrochemical reduction of oxygen in the separated electrodes and are considered as one of the ideal power sources for automotive and stationary applications due to their high energy efficiency, high power density, as well as low/zero emissions [1–3]. However, to become commercially available, hydrogen fuel cells have to overcome the barrier of high cost caused by the exclusive use of platinum and platinum-based precious metal catalysts in both hydrogen oxidation and oxygen reduction at the electrodes. Therefore, the numerous efforts have been focusing on developing non-precious metal catalysts or metal-free catalysts [4,5].

One of the most promising non-precious metal catalysts in hydrogen fuel cells is carbon-supported transition metals or their compounds, which have gained increasing attention due to their promising activity towards ORR, along with the utilization of abundant and inexpensive raw materials [6–8]. Since the ORR activity of cobalt phthalocyanine in the alkaline electrolyte was found in 1964 [9], transition metal macrocycle compounds have been the focus of transition metal-based catalysts, such as (Fe, Co)/(porphyrins, phthalocyanines) [10–12]. However, stability issues arose from catalyst structure decomposition in the presence of acid resulted in the loss of catalytic activity [13]. It was found that high-temperature heat treatment on metal macrocycle compounds can not only enhance the stability of the catalysts but also increase their catalytic activity significantly, despite the atomic configuration of macrocycle compounds was found to partially or entirely decompose [14–16], indicating that the expensive macrocycle compounds of transition metal are not requisite for getting catalytically active sites, but the nitrogen species in transition metals or carbon supports are significant [17–19].

Carbon nanomaterials are attractive materials for catalyst support in fuel cells due to their microstructure and novel properties such as nanometer size, high accessible surface area, good electronic conductivity and corrosion resistance. Since Gong et al., reported the high ORR activity of nitrogen-doped CNTs in 2009 [20], the doped carbon materials as either metal-free catalyst or catalyst supports have been one of the hottest topics in the catalysts of fuel cell. Nitrogen-doped carbons can be prepared either through post-treatment on the as-prepared carbons with nitrogen-containing agents such as urea, hydrazine hydrate, and so on [21–23], or direct carbonization of nitrogen-containing precursors such melamine, polyaniline, polypyrrole and so on [24–26]. The ORR activity of N-doped carbons relates not only the nitrogen amount but also the types of nitrogen containing functional groups [27,28], besides specific surface area, pore structure and conductivity of N-doped carbons [29]. The catalysts of N-doped carbons supported transition metal or compounds can be synthesized either through the heat-treatment of transition metal macrocycle compounds [30–32] or by loading transition metals on the doped carbons [33–36]. Generally, they both require a subsequent heat-treatment process to enhance the stability of catalysts [37–39]. These heat-treatment processes have been confirmed to result the formation of coordination of metal and nitrogen ($M\text{-}N_x$). Consequently, it has been recognized that the catalytic activity toward ORR mainly originates from the $M\text{-}N_x$ sites of catalysts [40–42].

However, the real catalytically active sites of these transition metal based catalysts are still on the controversy. Using the carbide-derived carbons as a template to prepare the ORR catalysts with and without transition metal elements, Jaouen et al., gave their evidence that the true ORR activity is from the nitrogen-carbon structure in the outer surface of the nitrided carbon layer [43]. Although N-doped carbon materials are exhibiting their advantages in ORR catalysis [44,45], they are not be fully identified as metal-free catalyst since even trace metal elements contained in carbon materials can probably catalyze the ORR. However, the residual metals in carbon materials are difficult to be removed completely [46].

In the studies on ORR catalysts, much more attentions have been paid on the active sites of ORR, which are either oriented to metal and metal compounds sites or nitrogen-containing sites [47]. However, it should also be noted that there are possible synergistic effects of the different active sites on ORR.

In this work, three kinds of catalysts of the cobalt and nitrogen co-doped CNTs, the cobalt doped CNTs and the nitrogen-doped CNTs were prepared, respectively. These catalysts have a common characteristic experiencing the heating treatment in high pure nitrogen gas at 800 °C. The ORR properties of catalysts were examined and compared. The results demonstrate that the catalyst of nitrogen and cobalt co-doped CNTs combines the active sites of the nitrogen containing functional groups, cobalt and cobalt oxides and $Co\text{-}N_x$ structure, therefore, exhibits the excellent performance of electrolytic ORR close to commercial Pt/C catalyst used in hydrogen fuel cells.

Experimental

Chemicals and regents

Pyrrole (C_4H_5N, C. P. grade, $\geq$ 99.8%), Ammonium Persulfate ($(NH_4)_2S_2O_8$, A. R. grade, $\geq$ 99.7%), Hydrochloric acid (HCl, 1 M), Cobalt nitrate hexahydrate ($Co(NO_3)_2 \cdot 6H_2O$, A. R. grade, $\geq$ 99. 7%), Sodium borohydride ($NaBH_4$, G. R. grade, $\geq$ 99.7%), Potassium hydroxide (KOH, A. R. grade, $\geq$ 99.7%), and Sodium hydroxide (NaOH, A. R. grade, $\geq$ 99.7%) were obtained from Sinopharm Chemical Reagent Co., Ltd. Ultrapure N_2 and O_2 (supplied by the Anshan Angang gas Limited Liability Company) were used for de-aeration and the oxygen reduction reaction tests, respectively. All the aqueous solutions were prepared with ultrapure water supplied by an ultrapure water system.

The catalysts were synthesized through the routes as shown in Fig. 1. The catalyst of nitrogen-doped carbon nanotubes (NCNTs) was prepared by using the technology of thermal conversion of polymer coating [48]. The polypyrroles coated CNTs (PPy@CNTs) were firstly prepared by in-situ chemical polymerization of pyrrole onto the CNTs. The PPy@CNTs as prepared were placed into a horizontal furnace

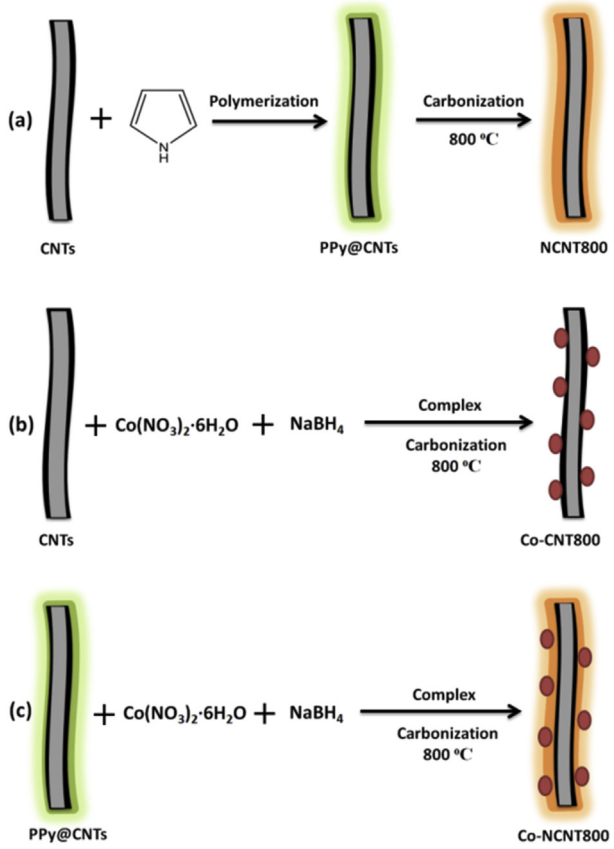

Fig. 1 – Schematic illustration of the catalysts synthesis.

and then the furnace was heating to 800 °C in high pure N_2 atmosphere with a rate of 10 °C min^{-1} and then the sample was kept at 800 °C for 1 h. The obtained sample is named as the NCNT800. The nitrogen and cobalt co-doped CNTs was prepared as following procedure, the PPy@CNTs of 200 mg and $Co(NO_3)_2 \cdot 6H_2O$ of 130 mg were ultrasonically dispersed in 50 mL deionized water and then the solution was heated to 80 °C and stirred magnetically for 0.5 h. And then the pH value of the solution containing PPy@CNTs was adjusted to 11 by using 0.1 M NaOH solution. After that 25 mL of 0.17 M $NaBH_4$ were dropped in the solution. The obtained solid product were filtered and washed several times by deionized water and then dried at 80 °C for 12 h in vacuum condition. Finally, the obtained black powders were heat-treated at 800 °C in high pure N_2 gas by using the same procedure as preparing the NCNT800, the sample was named as the Co-NCNT800. The cobalt doped CNTs were prepared as the same procedure of preparation the Co-NCNT800, but the replacing the PPy@CNTs by the same amount of CNTs as raw materials.

Sample characterization

The powder X-ray diffraction device (XRD, X'pret Powder, Rigaku D/MAX-2500X, Cu Kα), micro-Raman spectrometer (HORIBA Xplora Plus, excited by 532 nm lase) and the specific surface area (SSA) and pore structure analyzer (Micromeritics, ASAP2020) was used to characterize the composition and structure of samples. The SSA of samples was determined according to the Brunauer Emmett Teller (BET) method. The chemical states of samples were analyzed by X-ray photoelectron spectroscopy (XPS). The XPS was recorded with an ESCALAB250 surface analysis system using Al Kα radiation. The deconvolutions of the C 1s, N 1s and Co 2p spectra were performed using a non-linear least squares fitting program with a symmetric Gaussian function.

Electrochemical measurements

Electrochemical measurements were carried out in a conventional three-electrode cell filled with 0.1 M KOH solution at room temperature. A glassy carbon electrode (GCE) coated with the catalyst ink was used as the working electrode. A platinum plate with surface area (1 cm^2) was used the counter electrode. The Hg/HgO was chosen as the reference electrode. The GCE was polished by using the slurry of alumina (Al_2O_3, 0.3 and 0.05 μm), then rinsed thoroughly with ethanol and deionized water in an ultrasonic bath to remove any alumina residues. The catalyst ink was prepared by ultrasonic dispersing 10 mg of catalyst powder in 2 mL ethanol, into which 50 μL of 5 wt% nafion solution (DuPont) was added and the suspension as prepared was ultrasonically dispersed to get the homogenous solution. A quantity of 20 μL of the catalyst ink was pipetted out and dropped on the top surface of GCE, finally, the GCE coated with the catalyst ink was dried under a vacuum at 80 °C for 12 h.

Cyclic voltammogram (CV) and linear scan voltammetry (LSV) measurements were performed with an electrochemical analysis system of Reference 3000 workstation (Gamry Instruments, USA). The rotating disk electrode (RDE, RDE710 Rotating Electrode, Gamry Instruments, USA) coated with the catalysts was used for LSV tests. All potentials reported in this work were referenced to the reversible hydrogen electrode (RHE) , $E_{RHE} = E_{Hg/HgO} + 0.059\ pH + 0.098$.

Results and discussion

The XRD patterns of samples are shown in Fig. 2. The peaks around 2θ of 26.2° are corresponded to C (002) of carbon matrix

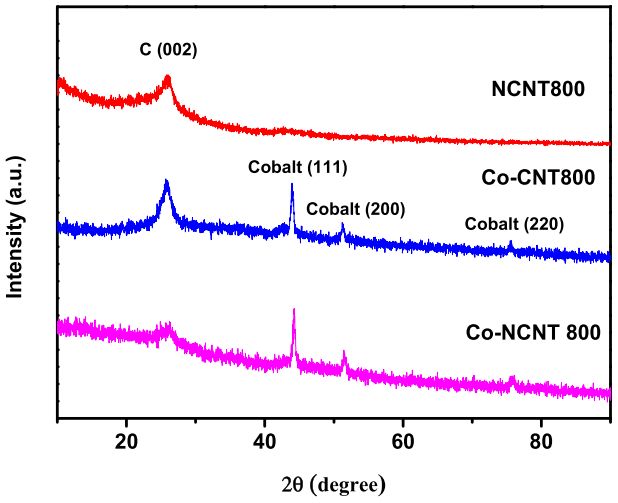

Fig. 2 – The XRD patterns of NCNT800, Co-CNT800 and Co-NCNT800.

for all the samples. The peaks around 2θ of 44.2°, 51.6° and 75.6° for the Co-CNT800 and Co-NCNT800 originate from the metallic cobalt of Co (111), Co (200) and Co (220), respectively. The cobalt is produced mainly through the reduction of Co^{3+} adsorbed on the carbon surface by the reducing agent of $NaBH_4$, and partially formed due to the carbothermal reduction reaction of the absorbed cobalt ions and cobalt oxides with carbons. It is easily noted that compared to the Co-CNT800, C (002) peak intensity of Co-NCNT800 become weak, which can be attributed to the nitrogen doped amorphous carbon layer on the CNTs, decreasing the graphitization degree of sample. This can be further confirmed by the Raman spectra of samples. Raman spectroscopy technique has been well demonstrated to characterize the degree of structural order of materials. As shown in Fig. 3D,G bands at 1350 cm^{-1} and 1590 cm^{-1} for the Co-CNT800 and Co-NCNT800 can be clearly seen, the latter shows more weak and broad peaks, probably due to the outer nitrogen doped amorphous carbon layer of sample decreasing scattering intensity, lightly. Since the D and G band reflects the defect and graphitization degree of carbon materials, respectively, the intensity ratio (I_D/I_G) can give us the structural order information of samples. The I_D/I_G is 1.36 and 1.43 for Co-CNT800 and Co-NCNT800, respectively, indicating that there are more defects in carbon matrix of Co-NCNT800. The more defects such as the edges of graphene along with nitrogen containing species in carbon matrix should enhance the activity for oxygen adsorption and thus probably improve the ORR performance of catalysts.

The N_2 adsorption-desorption isotherms of samples are shown in Fig. 4. All the isotherm belongs to type IV isotherm, at super low pressure ($P/P_0 < 0.1$), the adsorption volume of samples rise rapidly, indicating more micropores in the samples. The increase of adsorption volume at high relative pressure suggests a large mesoporous volume in the samples. The SSA and pore parameter of samples is listed in Table 1. The NCNT800 has the biggest SSA owing to the nitrogen doped porous carbon layer converted from the PPy coating containing more micropores. The Co-NCNT800 also exhibits relative higher SSA and microporous volume than the Co-CNT800,

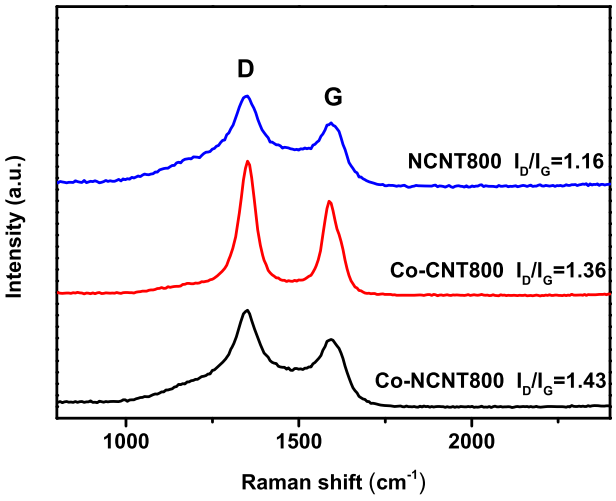

Fig. 3 – Raman spectra of NCNT800, Co-CNT800 and Co-NCNT800.

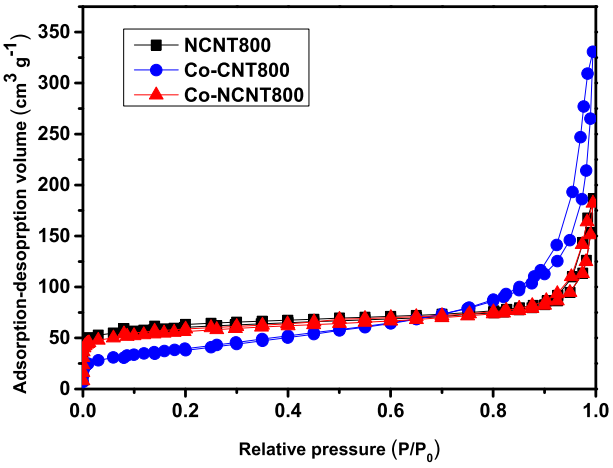

Fig. 4 – N_2 adsorption-desorption isotherms of samples.

since its support has the similar pore structure with the NCNT800.

X-ray photoelectron spectroscopy (XPS) is a useful tool to study the surface composition of materials. Fig. 5a is the XPS survey spectra of samples, the peaks around binding energy of 282.5, 398.5, 532.2 and 780.7 eV are assigned to C 1s, N 1s, O 1s and Co 2p. Table 2 gives the relative atomic percentage of C, O, N and Co of samples according to the XPS analysis results. The elemental cobalt content of Co-NCNT800 (1.37 at %) is much higher than the Co-CNT800 (0.42 at %), which can be attributed to the improved hydrophility and surface activity of NCNT support of Co-NCNT800 enhancing the deposition of cobalt or its compounds. It can be also noted that the higher oxygen content of the Co-NCNT800, which should arise from the higher cobalt oxides and oxygen containing species onto the surface of sample. The Co-NCNT800 has almost the same nitrogen content with the NCNT800, suggesting that cobalt doping does not influence the nitrogen amount of sample. The N 1s spectra of NCNT800 and Co-NCNT800 are shown in Fig. 5b, c. The peaks around the binding energy of 397.5, 400.1 and 401.5eV are assigned to pyridinic-N, pyrrolic-N and quaternary-N of both samples [49,50]. Significant difference between the two samples is that there is another peak around 399.5 eV arising from Co-N_x coordination structure [51] only for the Co-NCNT800, which is most probably produced by the co-doping of cobalt and nitrogen in the sample. Moreover, it worthy to note that the relative content of quaternary-N of Co-NCNT800 is much higher than the NCNT800 as shown in Table 3, indicating that the doping cobalt in the sample enhances the conversion of pyrrolic-N into quaternary-N. It had been demonstrated that the quaternary-N functional groups in the nitrogen doped carbon can supply the better activity toward ORR in our previous study [52].

The Co 2p spectrum of Co-CNT800 and Co-NCNT800 are shown in Fig. 5d, e. The cobalt with the different price states are the prominent surface composition of both samples. The peaks around the binding energies of 779.1, 780.2, 782.6, 784.7 and 795.6 eV (Co $2p_{1/2}$) are assigned to the Co_3O_4, CoO and Co_2O_3 species or their mixtures, the peak of binding energy at 803.0 eV maybe the presumable existence of CoO [42]. Especially, noting that a peak of the Co-N_x structure can be

Table 1 – Specific surface area and pore structure parameters of NCNT800, Co-CNT800 and Co-NCNT800.

Catalysts	BET specific surface area (m^2/g)	Total pore volume (cm^3/g)	Adsorption average pore width (nm)	Micropore volume (cm^3/g)
NCNT800	197.1	0.288	11.90	0.082
Co-CNT800	142.8	0.301	7.67	0.001
Co-NCNT800	153.7	0.283	10.57	0.024

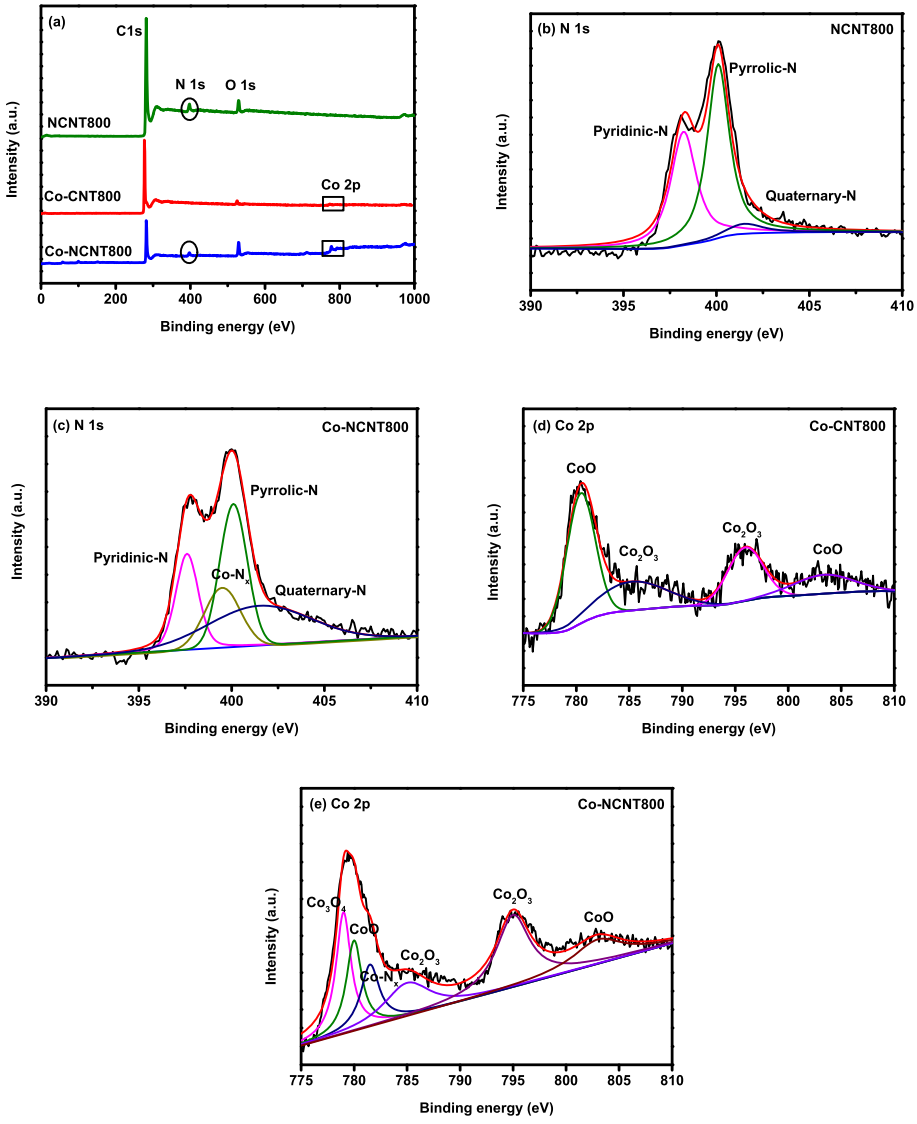

Fig. 5 – XPS survey spectra of the samples (a), N 1s of NCNT800 (b), N 1s of Co-NCNT800 (c), Co 2p of Co-CNT800 (d), Co 2p of Co-NCNT800 (e).

Table 2 – Surface elements content (at %) of the NCNT800, Co-CNT800 and the Co-NCNT800 according to XPS analysis.

Catalysts	C 1s	O 1s	N 1s	Co 2p
NCNT800	87.62	5.36	6.35	–
Co-CNT800	97.05	2.53	–	0.42
Co-NCNT800	79.27	13.16	6.20	1.37

Table 3 – Nitrogen containing functional groups content (at %) of the NCNT800 and the Co-NCNT800 according to XPS N 1s spectra analysis.

Catalysts	Pyridinic-N	Pyrrolic-N	Quaternary-N
NCNT800	41.00%	53.90%	5.10%
Co-NCNT800	36.85%	31.06%	32.09%

identified at bonding energy of 781.5 eV for the Co-NCNT800 sample [53]. The metal-N_x sites are often considered as the active sites of ORR [54]. Nevertheless, it shouldn't omit the catalytic effects of cobalt oxides on ORR [55]. As shown later, the Co-CNT800 with the surface composition only containing cobalt oxides still exhibits the observed ORR activity. The cobalt oxides should be formed due to the oxidation of surface of metallic Co since the exposed metallic cobalt interacts with aerobic atmosphere or a small amount of oxygen in the precursor.

The catalytic properties of samples toward ORR were analyzed by the electrochemical methods. Cyclic voltammograms (CV) of samples in 01.M KOH solution are shown in Fig. 6. The ORR peaks around the potential range of 0.6–0.9 V can be observed for the samples, indicating the ORR activity for the catalysts we prepared. It can be noted that the Co-NCNT800 owns the ORR peak potential of 0.861 V, which is much more positive than the NCNT800 (0.64 V) and the Co-CNT800 (0.66 V). Moreover, the Co-NCNT800 also exhibits much higher ORR peak current density than the other two samples. The ORR peak current density excluding the capacitive current is 0.273, 1.132 and 2.972 mA cm^{-2} for the NCNT800, Co-CNT800 and Co-NCNT800 in turns. Based on the CVs results, it can be concluded that the Co-NCNT800 owns the best ORR activity among samples. The ORR activity of NCNT800 arises mainly from the pyridinic-N and quaternary-N functional groups [56,57]. For the Co-CNT800, the cobalt oxides contribute the ORR activity. The Co-NCNT800 has not only pyridinic-N and quaternary-N, but also cobalt oxides, and additional Co-N_x coordination site. These active sites and their combination should give the Co-NCNT800 an excellent ORR property.

To further understand the ORR kinetics of the catalysts we prepared, the linear scan voltammetry (LSV) of samples in O_2-saturated 0.1 KOH solution was determined by using the rotating disk electrode (RDE) at room temperature. The LSV curves of samples as prepared and commercial Pt/C (20 wt%) catalyst tested at 1600 rpm are shown in Fig. 7a, the Co-NCNT800 owns much higher the limiting current density of oxygen diffusion (4.92 mA cm^{-2} at 0.2 V) and more positive the onset potential of ORR (1.06 V) than the samples of NCNT800 and Co-CNT800, which further confirms that the co-doping of cobalt and nitrogen can more significantly bring the sample ORR activity. Moreover, from the ORR onset potential and the limiting current, the Co-NCNT800 exhibits a comparable ORR performance with the commercial Pt/C catalyst whose onset potential and limiting current is 1.00 V and 5.16 mA cm^{-2}, respectively.

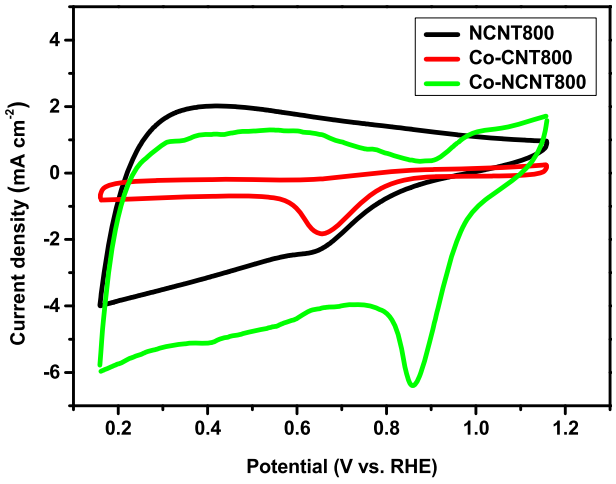

Fig. 6 – Cyclic voltammograms of NCNT800, Co-CNT800 and Co-NCNT800 in O_2-saturated 0.1 M KOH.

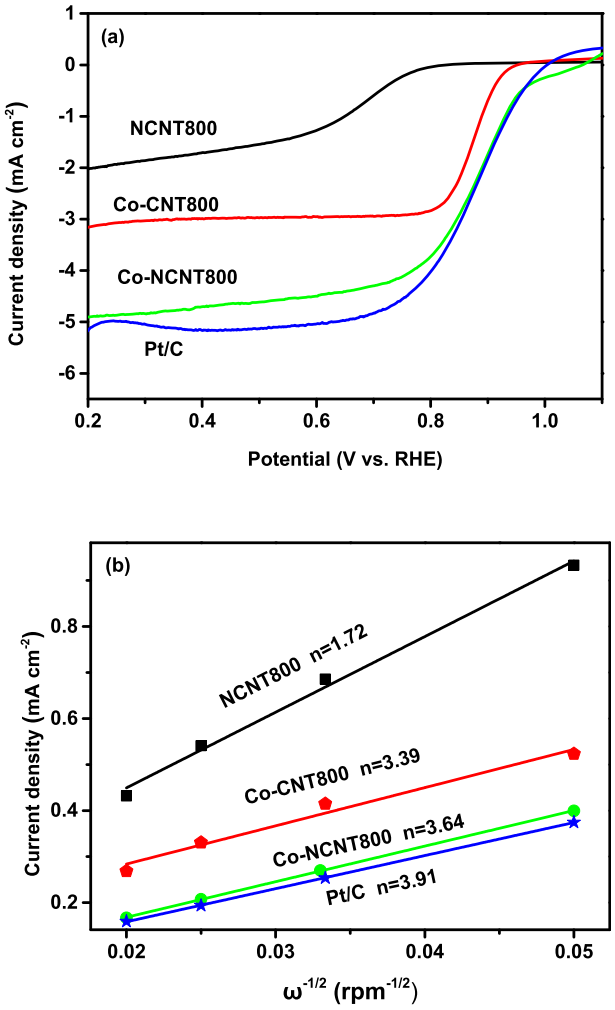

Fig. 7 – (a) LSV of samples in O_2-saturated 0.1 M KOH at 0.3 V with rotation rate 1600 rpm and (b) K-L plots and the transferred electron number of samples at 0.3 V.

The ORR mechanism based on electron transfer number was analyzed by using K-L equations [58]:

$$\frac{1}{J}=\frac{1}{J_K}+\frac{1}{J_L}=\frac{1}{J_K}+\frac{1}{B\omega^{1/2}}$$

$$B=0.2nFC_0D_0^{2/3}\upsilon^{-1/6}$$

$$J_K=nFkC_0$$

In the equations, J, J_K and J_L are the measured current density, kinetic current density and limiting diffusion current density, respectively. ω is the angular velocity of RDE, n is the total electron transfer number of ORR, F (96485 C mol^{-1}) is the

Faraday constant. In the 0.1 M KOH solution, the bulk concentration of oxygen is C_0 (1.9×10^{-5} cm^2 s^{-1}) and the diffusion coefficient of O_2 is D_0 (1.2×10^{-6} mol cm^{-3}). The linear K-L plots (J^{-1} vs $\omega^{-1/2}$) of all samples obtained from the LSVs at 0.3 V are shown in Fig. 7b. The transfer electrons number of ORR of NCNT800, Co-CNT800, Co-NCNT800 and 20% Pt/C is 1.72, 3.39, 3.64 and 3.91. Since the value of n suggests the dynamic mechanism of ORR, it can be deduced that, similar with commercial Pt/C catalyst, the Co-NCNT800 catalyzed ORR is mainly based on four-electron process.

Conclusions

Among the samples of the NCNTs, the cobalt doped CNTs and the cobalt and nitrogen co-doped CNTs we prepared, the Co-NCNT800 exhibits the best catalytic property toward ORR as the results demonstrated above. It can be concluded that the ORR activity of Co-NCNT800 is not only from the active species of cobalt oxides, nitrogen containing functional groups and Co-N_x coordination but also from the synergistic effects of these active species. These active species of ORR can be produced in the catalyst as the same time through the process of heating the composites of cobalt and PPy@CNTs, in which PPys can be converted into nitrogen containing functional groups, the cobalt oxides and the Co-N_x coordination can also be formed immediately. The simple preparation method and good ORR activity of our non-precious metal catalyst makes it promising in developing the hydrogen based fuel cells with high efficiency and low cost.

Acknowledgements

The financial supports from Natural Science Foundation of China (No. 51672118, 21701077 and 51872131), Department of Education of Liaoning province (No. 2017LNZD01) and Natural Science Foundation Project from Liaoning (No. 601009815_06) are gratefully acknowledged.

REFERENCES

[1] Demirdoven N, Deutch J. Hybrid cars now, fuel cell cars later. Science 2004;305:974–6.
[2] Duan JF, He YM, Zhu HR, Qin GL, Wei W. Research progress on performance of fuel cell system utilized in vehicle. Int J Hydrogen Energy 2019;44(11):5530–7.
[3] James K, Ram V, John JG, Jason M. Clean commercial transportation: medium and heavy duty fuel cell electric trucks. Int J Hydrogen Energy 2017;42(7):4508–17.
[4] Feng YJ, Nicolas AV. Nonprecious metal catalysts for the molecular oxygen-reduction reaction. Physica Status Solidi (b) 2008;245(9):1792–806.
[5] Bashyam R, Zelenay P. A class of non-precious metal composite catalysts for fuel cells. Nature 2006;443:63–6.
[6] Proietti E, Jaouen F, Lefevre M, Larouche N, Tian J, Herranz J, et al. Iron-based cathode catalyst with enhanced power density in polymer electrolyte membrane fuel cells. Nat Commun 2011;2:416.
[7] Lefevre M, Proietti E, Jaouen F, Dodelet JP. Iron-based catalysts with improved oxygen reduction activity in polymer electrolyte fuel cells. Science 2009;324:71–4.
[8] Liu BC, Dai WL, Liang ZX, Ye JS, Ouyang LZ. Fe/N/C carbon nanotubes with high nitrogen content as effective non-precious catalyst for oxygen reduction reaction in alkaline medium. Int J Hydrogen Energy 2017;42(9):5908–15.
[9] Jasinski R. A new fuel cell cathode catalyst. Nature 1964;201:1212.
[10] Wiesener K. N_4-chelates as electrocatalyst for cathodic oxygen reduction. Electrochim Acta 1986;31(8):1073–8.
[11] Zhang L, Song CJ, Zhang JJ, Wang HJ, Wilkinson DP. Temperature and pH dependence of oxygen reduction catalyzed by iron fluoroporphyrin adsorbed on a graphite electrode. J Electrochem Soc 2005;152:A2421–6.
[12] Song C, Zhang L, Zhang JJ, Wilkinson DP, Baker R. Temperature dependence of oxygen reduction catalyzed by cobalt fluoro-phthalocyanine adsorbed on a graphite electrode. Fuel Cells 2007;7(1):9–15.
[13] Alt H, Binder H, Sandstede G. Mechanism of the electrocatalytic reduction of oxygen on metal chelates. J Catal 1973;28(1):8–19.
[14] Van Der Putten A, Elzing A, Visscher W, Barendrecht E. Oxygen reduction on pyrolysed carbon-supported transition metal chelates. J Electroanal Chem Interfacial Electrochem 1986;205(1–2):233–44.
[15] Gupta S, Tryk D, Bae I, Aldred W, Yeager E. Heat-treated polyacrylonitrile-based catalysts for oxygen electroreduction. J Appl Electrochem 1989;19(1):19–27.
[16] You JM, Han HS, Lee HK, Cho S, Jeon S. Enhanced electrocatalytic activity of oxygen reduction by cobalt-porphyrin functionalized with graphene oxide in an alkaline solution. Int J Hydrogen Energy 2014;39(10):4803–11.
[17] Ohms D, Herzog S, Franke R, Neumann V, Wiesener K, Gamburcev S, et al. Influence of metal ions on the electrocatalytic oxygen reduction of carbon materials prepared from pyrolyzed polyacrylonitrile. J Power Sources 1992;38(3):327–34.
[18] Martins Alves CM, Dodelet JP, Guay D, Ladouceur M, Tourillon G. Origin of the electrocatalytic properties for oxygen reduction of some heat-treated polyacrylonitrile and phthalocyanine cobalt compounds adsorbed on carbon black as probed by electrochemistry and x-ray absorption spectroscopy. J Phys Chem 1992;96:10898–905.
[19] Arava LMR, Natarajan R, Sundara R. Cobalt-polypyrrole-multiwalled carbon nanotube catalysts for hydrogen and alcohol fuel cells. Carbon 2008;46(1):2–11.
[20] Gong KP, Du F, Xia ZH, Durstock M, Dai LM. Nitrogen-doped carbon nanotube Arrays with high electrocatalytic activity for oxygen reduction. Science 2009;323:760–4.
[21] Lin ZY, Waller G, Liu Y, Liu ML, Wong CP. Facile synthesis of nitrogen-doped graphene via pyrolysis of graphene oxide and urea and its electrocatalytic activity toward the oxygen-reduction reaction. Adv Energy Mater 2012;2(7):884–8.
[22] Bag S, Roy K, Gopinath CS, Raj CR. Facile single-step synthesis of nitrogen-doped reduced graphene oxide-Mn_3O_4 hybrid functional material for the electrocatalytic reduction of oxygen. ACS Appl Mater Interfaces 2014;6(4):2692–9.
[23] Lai LF, Potts JR, Zhan D, Wang L, Poh CK, Tang CH, et al. Exploration of the active center structure of nitrogen-doped graphene-based catalysts for oxygen reduction reaction. Energy Environ Sci 2012;5(7):7936–42.
[24] Choi CH, Chung MW, Park SH, Woo SI. Enhanced electrochemical oxygen reduction reaction by restacking of N-doped single graphene layers. RSC Adv 2013;3(13):4246–53.
[25] Sheng ZH, Shao L, Chen JJ, Bao WJ, Wang FB, Xia XH. Catalyst-free synthesis of nitrogen-doped graphene via

thermal annealing graphite oxide with melamine and its excellent electrocatalysis. ACS Nano 2011;5(6):4350–8.
[26] Li XL, Wang HL, Robinson JT, Sanchez H, Diankov G, Dai HJ. Simultaneous nitrogen doping and reduction of graphene oxide. J Am Chem Soc 2009;131(43):15939–44.
[27] Li JC, Hou PX, Shi C, Zhao SY, Tang DM, Cheng M, et al. Hierarchically porous Fe-N-doped carbon nanotubes as efficient electrocatalyst for oxygen reduction. Carbon 2016;109:632–9.
[28] Zhang JX, Lv MY, Liu DD, Du L, Liang ZX. Nitrogen-doped carbon nanoflower with superior ORR performance in both alkaline and acidic electrolyte and enhanced durability. Int J Hydrogen Energy 2018;43(9):4311–20.
[29] Liang J, Zhou RF, Chen XM, Tang YH, Qiao SZ. Fe-N decorated hybrids of CNTs grown on hierarchically porous carbon for high-performance oxygen reduction. Adv Mater 2014;26(35):6074–9.
[30] Baranton S, Coutanceau C, Roux C, Hahn F, Léger JM. Oxygen reduction reaction in acid medium at iron phthalocyanine dispersed on high surface area carbon substrate: tolerance to methanol, stability and kinetics. J Electroanal Chem 2005;577(2):223–34.
[31] Chen AL, Kong AG, Fan XH, Yang X, Li CL, Chen ZY, et al. High-efficiency copper-based electrocatalysts for oxygen electroreduction by heating metal-phthalocyanine at superhigh temperature. Int J Hydrogen Energy 2017;42(26):16557–67.
[32] Tiwari BR, Noori MT, Ghangrekar MM. Carbon supported nickel-phthalocyanine/MnO_x as novel cathode catalyst for microbial fuel cell application. Int J Hydrogen Energy 2017;42(36):23085–94.
[33] Liang YY, Li YG, Wang HL, Zhou JG, Wang J, Regier T, et al. Co_3O_4 nanocrystals on graphene as a synergistic catalyst for oxygen reduction reaction. Nat Mater 2011;10(10):780–6.
[34] Gao YY, Wang L, Li GZ, Xiao ZR, Wang QF, Zhang XW. Taming transition metals on N-doped CNTs by a one-pot method for efficient oxygen reduction reaction. Int J Hydrogen Energy 2018;43(16):7893–902.
[35] Jiang S, Zhu CZ, Dong SJ. Cobalt and nitrogen-cofunctionalized graphene as a durable non-precious metal catalyst with enhanced ORR activity. J Mater Chem A 2013;1(11):3593–9.
[36] Peng HL, Mo ZY, Liao SJ, Liang H, Yang LJ, Luo F, et al. High performance Fe- and N- doped carbon catalyst with graphene structure for oxygen reduction. Sci Rep 2013;3:1765.
[37] Wu G, More KL, Johnston CM, Zelenay P. High-performance electrocatalysts for oxygen reduction derived from polyaniline, iron, and cobalt. Science 2011;332:443–7.
[38] Xu P, Chen WZ, Wang Q, Zhu TS, Wu MJ, Qiao JL, et al. Effects of transition metal precursors (Co, Fe, Cu, Mn, or Ni) on pyrolyzed carbon supported metal-aminopyrine electrocatalysts for oxygen reduction reaction. RSC Adv 2015;5(8):6195–206.
[39] Zhang RZ, He SJ, Lu YZ, Chen W. Fe, Co, N-functionalized carbon nanotubes in situ grown on 3D porous N-doped carbon foams as a noble metal-free catalyst for oxygen reduction. J Mater Chem A 2015;3(7):3559–67.
[40] Dong L, Wang WP, Zang JB, Zhang Y, Wang ZY, Su J, et al. Fe, N codoped porous carbon nanosheets for efficient oxygen reduction reaction in alkaline and acidic media. Int J Hydrogen Energy 2018;43(31):14273–80.
[41] Wei Q, Zhang G, Yang X, Chenitz R, Banham D, Yang L, et al. 3D porous Fe/N/C spherical nanostructures as high-performance electrocatalysts for oxygen reduction in both alkaline and acidic media. ACS Appl Mater Interfaces 2017;9(42):36944–54.
[42] Wu ZS, Chen L, Liu JZ, Parvez K, Liang HW, Shu J, et al. High-performance electrocatalysts for oxygen reduction derived from cobalt porphyrin-based conjugated mesoporous polymers. Adv Mater 2014;26(9):1450–5.
[43] Jaouen F, Herranz J, Lefevre M, Dodelet JP, Kramm UI, Herrmann I, et al. Cross-laboratory experimental study of non-noble-metal electrocatalysts for the oxygen reduction reaction. ACS Appl Mater Interfaces 2009;1(8):1623–39.
[44] Li XB RY, Niu YY, Sun W, Tian XL. Synthesis of a N-doped mesoporous carbon as an efficient electrocatalyst for oxygen reduction. Int J Hydrogen Energy 2018;43(48):21791–7.
[45] Kadumudi FB, Balasubramaniyan R, Jin SC, Won MC. Facile synthesis of graphene/N-doped carbon nanowire composites as an effective electrocatalyst for the oxygen reduction reaction. Int J Hydrogen Energy 2015;40(21):6827–34.
[46] Masa J, Zhao AQ, Xia W, Sun ZY, Mei B, Muhler M, et al. Trace metal residues promote the activity of supposedly metal-free nitrogen-modified carbon catalysts for the oxygen reduction reaction. Electrochem Commun 2013;34:113–6.
[47] Li M, Bai L, Wu S, Wen X, Guan J. Co/CoO_x nanoparticles embedded on carbon for efficient catalysis of oxygen evolution and oxygen reduction reactions. ChemSusChem 2018;11(10):1722–7.
[48] An BG, Xu SF, Li LX, Tao J, Huang F, Geng X. Carbon nanotubes coated with a nitrogen-doped carbon layer and its enhanced electrochemical capacitance. J Mater Chem A 2013;1(24):7222–8.
[49] Li JC, Zhao SY, Hou PX, Fang RP, Liu C, Liang J, et al. A nitrogen-doped mesoporous carbon containing an embedded network of carbon nanotubes as a highly efficient catalyst for the oxygen reduction reaction. Nanoscale 2015;7(45):19201–6.
[50] Ratso S, Sahraie NR, Sougrati MT, Käärik M, Kook M, Saar R, et al. Synthesis of highly-active Fe–N–C catalysts for PEMFC with carbide-derived carbons. J Mater Chem A 2018;6(30):14663–74.
[51] Chen SM, Cheng JY, Ma LT, Zhou SK, Xu XW, Zhi CY, et al. Light-weight 3D Co-N-doped hollow carbon spheres as efficient electrocatalysts for rechargeable zinc-air batteries. Nanoscale 2018;10(22):10412–9.
[52] Li LX, Zhao HW, Xing TY, Geng X, Song RF, An BG. Nitrogen-doped carbon coatings on carbon nanotubes as efficient oxygen reduction catalysts. N Carbon Mater 2017;32(5):419–26.
[53] Jiang YY, Lu YZ, Wang XD, Bao Y, Chen W, Niu L. A cobalt-nitrogen complex on N-doped three-dimensional graphene framework as a highly efficient electrocatalyst for oxygen reduction reaction. Nanoscale 2014;6(24):15066–72.
[54] Qiao JL, Xu L, Liu YY, Xu P, Shi JJ, Liu SY, et al. Carbon-supported co-pyridine as non-platinum cathode catalyst for alkaline membrane fuel cells. Electrochim Acta 2013;96:298–305.
[55] Xu JB, Gao P, Zhao TS. Non-precious Co_3O_4 nano-rod electrocatalyst for oxygenreduction reaction in anion-exchange membranefuelcells. Energy Environ Sci 2012;5(1):5333–9.
[56] Li HB, Kang WJ, Wang L, Yue QL, Xu SL, Wang HS, et al. Synthesis of three-dimensional flowerlike nitrogen-doped carbons by a copyrolysis route and the effect of nitrogen species on the electrocatalytic activity in oxygen reduction reaction. Carbon 2013;54:249–57.
[57] Kim H, Lee K, Woo SI, Jung Y. On the mechanism of enhanced oxygen reduction reaction in nitrogen-doped graphene nanoribbons. Phys Chem Chem Phys 2011;13(39):17505–10.
[58] Xu F, Wang DQ, Sa BS, Yu Y, Mu SC. One-pot synthesis of Pt/CeO_2/C catalyst for improving the ORR activity and durability of PEMFC. Int J Hydrogen Energy 2017;42(18):13011–9.